Tidal controls on the flow of ice streams

Sebastian H. R. Rosier,[1] G. Hilmar Gudmundsson ,[1]

Corresponding author: Sebastian Rosier, British Antarctic Survey, Cambridge, UK. (s.rosier@bas.ac.uk)

[1]British Antarctic Survey, High Cross,

Madingley road, Cambridge, UK

The flow of many Antarctic ice streams is known to be significantly influenced by tides. In the past, modelling studies have implemented the tidal forces acting on a coupled ice-stream/ice-shelf system in a number of different ways, but the consequences that this has on the modelled response of ice streams to tides have, until now, not been considered. Here we investigate for the first time differences in model response that are only due to differences in the way tidal forcings are implemented. We find that attempts to simplify the problem by neglecting flexural stresses are generally not valid and forcing models with only changes in ocean back-pressure will not capture either the correct amplitudes or length scale.

1. Introduction

Ocean tides are known to significantly affect flow of ice streams over long distances upstream of the grounding line [*Anandakrishnan et al.*, 2003; *Bindschadler*, 2003; *Gudmundsson*, 2006; *King et al.*, 2010]. On Rutford Ice Stream (RIS), for example, tidally-induced motion causes periodic changes in surface velocity on the order of 10% over distances of tens of kilometers [*Gudmundsson*, 2006], and on the ice plain of Whillans Ice Stream (WIS) a pronounced stick-slip pattern in ice motion is observed in response to tides [*Bindschadler*, 2003] and diurnal variations in seismicity and strain observed over 300km upstream from the grounding line [*Harrison*, 1993].

Modelling work has shown that tidal modulation in the flow of ice streams depends on mechanical conditions at the glacier bed. The tidal variation in the flow of RIS can not, for example, be reproduced using linear sliding laws [*Gudmundsson*, 2011; *Rosier et al.*, 2015], and the stick-slip motion on WIS implies a plastic till rheology [*Bindschadler*, 2003; *Goldberg et al.*, 2014]. Observing and modelling tidally-induced motion in ice-stream flow therefore provides constraints on the basal sliding law, constraints that are difficult if not impossible to obtain in any other manner. Currently, no other approach is known that gives as direct an insight into the mechanical conditions on the base of active ice streams as that of validating numerical models against observations of tidally-induced variations in flow.

To date, the prime aim of modelling studies of tidally-induced variation in the flow of ice streams has been to identify the physical mechanisms responsible for the observed response. As with all such modelling work, the model output depends both on various

aspects of the model itself as well as on the model forcings. The modelled response to tidal forcing is therefore always dependent on both the physical description of ice-stream flow used, as well as the type of tidal forcing applied to the model. One might expect the input, i.e. the tidal forcing itself, to be a sufficiently well understood process for all modelling approaches to have applied identical, or at least very similar, tidal forcings. To the contrary however, published numerical models of ocean-induced tidal variations have to date used very different tidal forcing parameterizations. In some cases, the differences are so large that there is hardly any overlap between those descriptions. For example, some numerical models have accounted for the change in ocean pressure acting horizontally due to varying ocean height [e.g. *Bindschadler*, 2003; *Thompson et al.*, 2014], but at the same time not included stresses set up in the ice by tidal flexure. Other models have only included the flexural stresses [e.g. *Gudmundsson*, 2007; *King et al.*, 2010, 2011], and ignored the changes in ocean pressure acting horizontally.

Here we use numerical modelling to clarify the respective impacts of different types of tidal forcings, and to quantify their relative importance to ice-stream motion. Our focus is on long-range effects of tides on ice-stream motion, i.e. on processes having the potential to significantly impact horizontal motion (e.g. perturbations greater than about 10 % of mean flow velocity) over spatial scales that are large compared to the mean ice thickness around the grounding line. We will therefore, for example, not attempt to replicate details of vertical flexural profiles around grounding lines, but we are interested in quantifying the effect that tidal flexure can have on horizontal ice flow velocities upstream of the grounding line over distances large compared to mean ice thickness

Motivated by past modelling approaches we distinguish between three different types of tidal forcings: 1) *damming stresses*, i.e. temporal variations in horizontal stresses at the grounding line arising from tidal variation in water depth, 2) *flexural stresses*, which are the stresses set up by the flexure of the ice around the grounding line as the ice shelf moves up and down with the ocean tides, and 3) *hydrological tidal forcing*, which are pressure variations in the subglacial drainage system upstream of the grounding line, driven by variations in ocean pressure.

Our main purpose is to determine the relative importance of damming and flexural stresses on ice-stream motion (see Fig.1), and furthermore to test if omitting either the damming or flexural stresses, as has been done in a number of previous studies, is justified. We then compare the relative importance of these two types of tidal forcings on ice flow velocities, to those caused by hydrological tidal processes as recent work [*Thompson et al.*, 2014; *Rosier et al.*, 2015] suggests that in some cases this is the primary mechanism giving rise to tidally-induced velocity variations on ice streams. We note that there are further possible types of tidal forcings, tidal migration of the grounding line being one such example, and these have been studied in a number of recent papers [*Sayag and Worster*, 2013; *Rosier et al.*, 2014; *Tsai et al.*, 2015].

As explained in detail below we find, for all cases that we study, tidal damming stresses to have less impact on ice-stream flow than tidal flexural stresses, and these both in turn to have a smaller effect than tidal hydrological forcing. This finding cast doubts over a number of models used in the past where damming stresses where the only type of tidal forcing considered.

2. Methodology

We use the full-Stokes nonlinear visco-elastic model of *Rosier et al.* [2015] to run simulations in which flexural stresses (F), damming stresses (D) and hydrology (H) are either included or neglected. Our aim is to investigate the relative importance of these three types of tidal forcings on ice-stream flow. A description of the numerical model can be found in Appendix A or in more detail in *Rosier et al.* [2015]. As explained in *Rosier et al.* [2015] the model has been shown to accurately reproduce tidal variations in ice flow observed at RIS, West Antarctica.

Flexural stresses are generated through the flexure of the ice shelf [e.g. *Holdsworth*, 1969; *Reeh et al.*, 2003], and in experiments where those stresses are not desired we remove the ice-shelf portion of the model domain. Damming stresses can be removed from the model by only including the vertical component of the ocean pressure force beneath the ice shelf. Hydrology, implemented by perturbing basal water pressure at tidal timescales, was found to be a key mechanism to explain observations on the RIS [*Rosier et al.*, 2015] but we also undertake simulations where the basal water pressure does not vary as might be the case in other ice streams or tidewater glaciers. More details of how each parameterization is implemented within the model can be found in Appendix A. Runs are named according to the processes included, for example a simulation with hydrology and flexural stresses but not damming stresses is denoted H + F.

The tidal constituents used to generate the time-dependent external tidal forcings are taken from the CATS2008 tidal model [*Padman et al.*, 2008]. Direct GPS measurements have shown this tidal model to perform well in the region around RIS [*Gudmundsson*,

2007]. In total we included four semi diurnal (M_2, S_2, K_2 and N_2) and two diurnal (O_1, K_1) tidal components that comprise the six largest constituents at the RIS grounding line. No long-periodic tidal components were included in the forcing as both direct GPS measurements and the CATS2008 model show these to be insignificant in comparison.

3. Results

Our main measure of the effects of the F, D and H tidal forcings on ice-stream motion are the amplitudes and the phase shifts of periodic variations in (horizontal) surface flow speeds at different tidal frequencies. We focus here primarily on the semidiurnal M_2 and the fortnightly M_{sf} tidal components (with periods of 0.516 and 14.77 days respectively). The fortnightly M_{sf} component was chosen because on a number of ice streams, e.g. RIS, the strongest response is at this frequency [*Gudmundsson*, 2006; *King et al.*, 2010], and also because this long-period modulation in flow can only be generated through some nonlinear mechanism [*Gudmundsson*, 2007].

The numerical model was run with some of the modelled tidal forcings (i.e. F, D and H) either included or excluded to determine their relative importance. Figure 2 shows the amplitudes of tidal components M_{sf} and M_2 as functions of distance upstream from the grounding line. These were obtained by detrending horizontal surface displacements and then extracting the tidal frequencies using the t_tide matlab package [*Pawlowicz et al.*, 2002].

In Fig. 2 the results are arranged such that results for all combinations of tidal forcings (F, D and H) are shown together in the left-hand panels. Because the effect of tidally-induced subglacial water pressure variations is so large in comparison to other types of

tidal forcings, we show again in the right-hand panels those results not involving the type H forcing. It is important to note that the response to the H forcing is large in this case due to the choice of hydrological parameters that were made in order to match observations on the RIS, and these may not be applicable on other ice streams.

Focusing on those results not involving the H forcing (panels b and d in Fig. 2), the most striking contrast between the response to the F and D forcings is the difference in resulting long-period M_{sf} amplitudes. As panel b of Figure 2 shows, the D tidal forcing produces, in comparison to the F tidal forcing, almost no tidal response at the M_{sf} frequency. We find when combining D with F, the resulting M_{sf} amplitudes to be similar to those arising from F alone (yellow curve in panel d of Fig. 2). On the other hand the short-periodic M_2 response to both F and D is similar (see panel d of Fig. 2). Hence, the F and D forcings differ sharply in their ability to generate M_{sf} amplitudes, and models that included only D and not the H tidal forcing may therefore significantly underestimate the long-periodic impact of tides. This is assuming that such models are capable of generating long-periodic response from short-periodic tidal forcing at all. Even when F tidal forcing is included, any linear model will never generate any response at the M_{sf} frequency [*Gudmundsson*, 2007].

To investigate further the reasons why the F tidal forcing generates so much larger M_{sf} amplitudes than the D type, we look at differences in viscous and elastic response to those two tidal forcings. In Figure 3 detrended basal viscous (top panel) and elastic (lower panel) shear strains (ϵ_{xy}) 20 km upstream from the grounding line are plotted for both D and F forcings. As the figure shows, elastic strains generated by the D and

F tidal forcings are similarly large and approximately in phase (blue and red curves in lower panel of (Fig. 3). Viscous strains generated by the D and the F tidal forcings are, however, qualitatively and quantitatively very different. Those generated by the F forcing are not only several times larger than those generated by the D tidal forcing, but also show marked long-periodic variation with time that is mostly absent in the D response . The F tidal forcing is able to generate large perturbations in basal shear stresses, which, when coupled with a nonlinear viscous sliding law, gives rise to a nonlinear response in basal shear strains.

We now consider the impact of tides on subglacial water pressure and the resulting effects on ice-stream motion. When this hydrological tidal forcing (H) is applied (panels a and c, solid lines in Fig. 2), resulting M_{sf} amplitudes are increased at least five-fold. This strong response to the H, as compared to both the D and F forcings, was already noticed by [*Rosier et al.*, 2015], where it was concluded that observed M_{sf} amplitudes on RIS cannot be reproduced without including the H forcing type. Further adding tidal damming to the hydrological forcing (H + D) *reduces* M_{sf} amplitude, as does adding flexural stresses (H + F). Both of these M_{sf} amplitude reductions are consequences of differences in phase between the response to H as compared to D and F. Inspecting our model results we found the phases of the D and F responses to be opposite to that from H, resulting in a deconstructive interference between H and D and between H and F. This same effect can also be seen clearly in panel c, where adding F and D to H reduces M_2 amplitudes as compared to applying the H tidal forcing alone.

4. Discussion

A comparison between simulations that include only flexural stresses and only tidal damming stresses shows that the former is almost entirely responsible for the generation of long-period modulation in flow when hydrological affects are neglected. The key difference between the two processes is that the basal shear stresses generated through flexure are over an order of magnitude larger than the tidal damming stresses at the grounding line. When coupled with a nonlinear sliding law these basal shear stress perturbations then, in turn, give rise to long-periodic modulation in ice flow.

Although not used within the model, it is helpful to think of flexural stresses in terms of the analytical solution for an elastic beam. Longitudinal flexural stresses (σ_{xx}, positive in tension) generated by bending of a floating ice tongue were given by *Holdsworth* [1969] as

$$\sigma_{xx}(z', x) = -\frac{6\rho_{\mathrm{w}} g z' S(t)}{H^3 \lambda^2} e^{-\lambda x}(\cos(\lambda x) - \sin(\lambda x)), \tag{1}$$

where λ is the bending length scale

$$\lambda^4 = \frac{3\rho_w g(1-\nu^2)}{EH^3}, \tag{2}$$

$z' = z - s + \frac{H}{2}$ (with z pointing upwards such that $z = 0$ at mean sea level and $z = s$ at the ice surface), H is ice thickness, E is the Young's modulus, ν is the Poisson's ratio, ρ_w is water density, $S(t)$ is the change in mean sea level due to the ocean tides and λ is the bending length scale. The equation above shows that $\sigma_{xx} \propto 1/\sqrt{H}$ and $\sigma_{xx} \propto A$ where A is the tidal amplitude (i.e. the maximum of $S(t)$). In the case of the RIS ($H \approx 2000, A \approx 3$) flexural stresses are expected to be over two times larger than along the Siple Coast, whose ice streams are quite different in thickness and tidal forcing ($H \approx 1000, A \approx 1$).

Variation in tidal forcing around Antarctica therefore plays the most important role in determining the magnitude of flexural stresses. While we predict flexural stresses to be larger for the RIS than Siple Coast ice streams, the relation above shows that this is *in spite* of its greater thickness and thus for thinner ice streams (with a floating ice shelf) damming stresses are expected to be even less important than we have shown here.

Solutions to Eq.1 take the form of damped harmonic oscillations, with the longitudinal stress reversing sign at characteristic distances upstream from the grounding line [*Holdsworth*, 1969]. At the grounding line, flexural stresses cause horizontal compression at the upper ice surface at high tide and horizontal extension at the ice-till interface. These basal stresses are reduced and then become compressive with increasing distance upstream. This stress reversal is the reason why basal shear strain is in phase with the tide at the grounding line but out of phase further upstream beyond the turning point. In the case of damming stresses the situation is in comparison fairly simple; at high tide the damming stresses are largest, leading to a minimum in velocity, such that at the grounding line the shear strain is approximately 180° out of phase with the tide. The result is that, sufficiently far away from the grounding-line, phases of surface velocities are broadly similar for both D and F types of tidal forcings. A consequence of flexural stresses reversing sign and becoming zero at points upstream of the grounding line is a minimum in the M_2 component of horizontal motion that can be seen in Fig. 2d for simulations that include the F forcing.

In some ways the simulations with no flexural stresses can be considered analogous to tidewater glaciers where there is no floating ice shelf. However, for tidewater glaciers

the boundary condition (A5) is not strictly correct. To check the effect of the different boundary condition, the model was re-run for this alternative situation whereby an ocean pressure force acts on the ice front below sea level. While the mean stresses at the ice front are different in this case, the perturbations by tidal damming stresses are the same and the tidal response within the model is almost identical. We can therefore say with confidence that tidewater glaciers will not generate long-period modulation in ice flow unless they are close to flotation and the subglacial water pressure is modulated by ocean tides.

Thompson et al. [2014] used a full-Stokes model and investigated forcing it with and without flexure in an attempt to justify ignoring flexural stresses in the majority of their simulations. As the authors themselves point out, flexural stresses as calculated using the elastic beam approach are expected to be an order of magnitude greater at the grounding line than damming stresses. Their approach is to consider the length scales of tidal stress perturbations and the model does not explicitly generate a long-period response. While it is true that the length scales of the two mechanisms are similar, it is clear from the results presented here that their respective amplitudes play an important role in generating long-period modulation in ice flow. The key point is that the length scale of the generated M_{sf} modulation in ice flow, which operates at a dominantly viscous timescale, is much longer than the dominantly elastic mechanisms that generate it. Contrary to *Thompson et al.* [2014] we do not find that the length scale is the limiting factor in matching observations within our model, but tidal stresses alone are not large enough to generate the M_{sf} signal seen on the RIS. In this respect hydrology remains the key ingredient that can produce

a large enough surface signal, as first suggested by *Thompson et al.* [2014], however this has only been shown for the RIS and it may be that on other ice streams there is little or no effect from tidally varying hydrology.

We chose not to include grounding-line migration due to the tides in this model, our goal here is only to compare the relative importance of tidal damming and flexural stresses. A previous version of the model did include this process as a contact problem [*Rosier et al.*, 2014] and lower order models can also include this [*Sayag and Worster*, 2013]. Migration distance is very sensitive to bed slope and since this is not well constrained we prefer to avoid this complication. It is likely that adding this process would slightly reduce flexural stresses, however it is difficult to see how it would reduce them to such an extent that they are of equal or smaller magnitude than tidal damming stresses.

Previous studies of tidal modulation of ice-stream flow have often neglected flexural stresses. Vertically integrated models are often used and forced with tidal damming stresses and/or GPS measured velocities. Given that these models do not include the most important physics their value in shedding light on the mechanisms of ice-stream flow is questionable. In reality these observations of tidal modulation are hard to reproduce without using a full-Stokes model when all the competing stresses are included.

5. Summary and Conclusions

Using a three-dimensional nonlinear visco-elastic model, that has been shown to be able to replicate observations of tidally-induced motion on Rutford Ice Stream, West Antarctica, we have conducted a sensitivity study of the impacts of different types of

tidal forcings on ice stream flow. We distinguish between three different types of tidal forcings: damming (D), flexural (F), and hydrological (H).

When comparing the relative impacts of D and F forcings in our model, we find the D forcing type to have much smaller impact on ice-stream flow. In nature the D and the F type forcings are simply different aspects of the same tidal mechanism acting on ice-streams. We conclude that it is a mistake to only include the D part while ignoring the F part, and we question the relevance of models studies done in the past that have done so.

In an earlier study [*Rosier et al.*, 2015] we found that observations on Rutford Ice Stream could not be replicated for any parameter values using only the D and the F tidal forcings, and that an additional forcing type, i.e. H forcing, had to be included. Here we find that the D and F forcings act deconstructively in combination with the H forcing. This is seen in both the short (M_2) and the long (M_{sf}) periodic response. The magnitude of this deconstructive interference decreases rapidly with distance upstream from the grounding line. Further observations will allow us to determine if H-type forcing is generally the single most important tidal forcing mechanism on ice streams, as it is for the RIS, and this can only be done on a case by case basis.

We acknowledge that due to our numerical approach it is difficult, if not impossible, to provide a fully general statement about the relative importance of different types of tidal forcings for all glacier geometries. Nevertheless, because differences in response to our three types of tidal forcings are large and because flexural stresses are in general expected to be larger for thinner ice streams, we do expect our results to be relatively insensitive

to changes in ice-stream geometry. In this way, for any thickness of ice stream with an adjoining floating shelf, modelling the tidal response as a result of damming stresses alone ignores an important aspect of the mechanical forcing and will not capture either the correct amplitudes or length scale.

Appendix A: Model Description

We use the full-Stokes finite element software MSC.Marc [*MARC*, 2014] that treats ice as a visco-elastic body, as described in detail in [*Gudmundsson*, 2011; *Rosier et al.*, 2014, 2015]. This solves the field equations for the conservation of mass, linear momentum and angular momentum:

$$\frac{D\rho}{Dt} + \rho v_{i,i} = 0 \tag{A1}$$

$$\sigma_{ij,j} + f_i = 0 \tag{A2}$$

$$\sigma_{ij} - \sigma_{ji} = 0 \tag{A3}$$

where D/Dt is the material time derivative, ρ is density, ν_i are the components of the velocity vector, σ_{ij} are the components of the Cauchy stress tensor and f_i are the components of the gravity force per volume. A Maxwell rheological model is used, whereby deviatoric strain rate is the sum of elastic and viscous terms. The elastic modulus (E) and Poisson's ratio (ν) used in all model simulations were 4.8 GPa and 0.41 respectively, as these values have been shown to best match tidal observations for viscoelastic models [*Reeh et al.*, 2003; *Gudmundsson*, 2011].

The model is 120km long (100km grounded, 20km floating) and 16km wide, apart from simulations without an ice shelf in which case the floating portion is removed. Along

one sidewall we apply a no-slip condition and the other sidewall a free-slip condition, representing the ice stream medial line to give a total width of 32km.

Where an ice shelf is present we apply an oceanic pressure acting normal to the base of the shelf, given by

$$p_w = \rho_{\mathrm{w}} g(S(t) - z). \tag{A4}$$

As the ice shelf bends, some of this force is resolved in the horizontal direction, leading to an increase in damming stresses at high tide and reduction at low tide. At the upstream boundary of the model we apply the cryostatic pressure $p = \rho_{\mathrm{i}} g(s - z)$ normal to the ice.

At the downstream boundary most simulations (except for the case of a tidewater glacier that is discussed briefly) apply the following boundary condition to the ice front:

$$\sigma_{xx} = -\rho_{\mathrm{i}} g(s - z) + \frac{\rho_{\mathrm{i}} g H}{2}\left(1 - \frac{\rho_{\mathrm{i}}}{\rho_{\mathrm{w}}}\right) - p_b, \tag{A5}$$

where p_b is buttressing.

Flexural stresses are normally already in the model, but the aim of some simulations is to examine ice-stream response to a tidal forcing where these stresses are absent. This is done by removing the ice shelf portion of the model domain. Since the oceanic pressure acting on the base of the shelf no longer produces a damming force this is applied by adding a tidally varying pressure component $\rho_{\mathrm{w}} g S(t)$ to equation A5.

Upstream from the grounding line along the ice-bed interface we use a sliding law of the form

$$u_b = c' \frac{\tau_b^m}{(1 + \xi)^q}, \tag{A6}$$

where $c' = c\overline{N}^{-q}$, $\xi = \Delta N / \overline{N}$, $\Delta N = -\rho_w g h$, $\overline{N}$ is mean effective pressure, c is slipperiness, τ_b is basal shear stress, h is hydraulic head and m and q are constants.

Runs without any tidally-varying subglacial pressure simply set $\Delta N = 0$ such that Equation A6 reduces to the more common form e.g. *Budd and Keage* [1979]; *Bindschadler* [1983]. In simulations where hydrology is perturbed by the tides, hydraulic head at the grounding line is equal to the change in mean sea level and this is transmitted upstream through a diffusion process such that $\partial_t h = K\partial_{xx} h$ where K is the hydraulic diffusivity.

A formal Bayesian inversion is done to obtain the slipperiness distribution ($c'(x)$) and buttressing that best match observed medial line velocities, as described fully in *Rosier et al.* [2015]. All parameter choices are the same as in recent modelling work, chosen so that they best match long-period modulation in ice stream flow for the default simulation with all processes included e.g. H + D + F (table 1).

Acknowledgments. The authors would like to thank the two anonymous reviewers of this manuscript for their constructive comments. This work was partly supported by the NERC large grant 'Ice shelves in a warming world: Filchner Ice Shelf system' NE/L013770/1.

References

Anandakrishnan, S. and Voigt, D. E. and Alley, R. B.: Ice stream D flow speed is strongly modulated by the tide beneath the Ross Ice Shelf, Geophys. Res. Lett., *30*, 1361, doi: 10.1029/2002GL016329, 2003.

Bindschadler, R. (1983), The importance of pressurized subglacial water in separation and sliding at the glacier bed, *Journal of Glaciology*, *29*(101), 3–19.

Bindschadler, R. A., King, M. A., Alley, R. B., Anandakrishnan, S., and Padman, L.: Tidally controlled stick-slip discharge of a West Antarctic ice stream, *Science*, 301, 10871089, 2003a.

Budd, W. F., and P. L. Keage (1979), Empirical studies of ice sliding, *Journal of glaciology*, *23*(89), 157–170.

Gudmundsson, G. H. (2006), Fortnightly variations in the flow velocity of Rutford Ice Stream, West Antarctica., *Nature*, *444*(7122), 1063–4, doi:doi:10.1038/nature05430.

Gudmundsson, G. H. (2007), Tides and the flow of Rutford Ice Stream, West Antarctica, *J. Geophys. Res.*, *112*, F04,007, doi:10.1029/2006JF000731.

Gudmundsson, G. H. (2011), Ice-stream response to ocean tides and the form of the basal sliding law, *The Cryosphere*, *5*(1), 259–270, doi:10.5194/tc-5-259-2011.

Goldberg D, Schoof C, and O. Sergienko (2014) Stick-slip motion of an Antarctic Ice Stream: the effects of viscoelasticity. *J. Geophys. Res. Earth Surface. 119* (7),1564–1580.

Harrison, W. D.: Short-period observations of speed, strain and seismicity on Ice Stream B, Antarctica , J. Glaciol., *39*, 463–470, 1993.

Holdsworth, G. (1969), Flexure of a floating ice tongue, *J. Glaciol.*, *8*, 133–397.

King, M. A., T. Murray, and A. M. Smith (2010), Non-linear responses of Rutford Ice Stream, Antarctica, to semi-diurnal and diurnal tidal forcing, *J. Glaciol.*, *56*(195), 167–176, doi:10.3189/002214310791190848.

King, M. A., K. Makinson, and G. H. Gudmundsson (2011), Nonlinear interaction between ocean tides and the Larsen C Ice Shelf system, *Geophys. Res. Lett.*, *38*(8), 1–5, doi:

10.1029/2011GL046680.

MARC (2014), *Marc 2014 user manual*, MSC Software Corporation, 2 MacArthur Place, Santa Ana, CA 92707, USA.

Padman, L., Erofeeva, S. Y., and Fricker, H. A.: Improving Antarctic tide models by assimilation of ICESat laser altimetry over ice shelves, Geophys. Res. Lett., *35*, L22504, doi:10.1029/2008gl035592, 2008.

Pawlowicz, R., B. Beardsley, and S. Lentz (2002), classical tidal harmonic analysis including error estimates in matlab using t_tide, *Computers and Geosciences*, *28*, 929–937.

Reeh, N., E. L. Christensen, C. Mayer, and O. B. Olesen (2003), Tidal bending of glaciers: a linear viscoelastic approach, *Ann. Glaciol.*, *37*, 83–89, doi: 10.3189/172756403781815663.

Rosier, S. H. R., G. H. Gudmundsson, and J. A. M. Green (2014), Insights into ice stream dynamics through modeling their response to tidal forcing, *The Cryosphere*, *8*, 1763–1775, doi:10.5194/tc-8-1763-2014.

Rosier, S. H. R., G. H. Gudmundsson, and J. A. M. Green (2015), Temporal variations in the flow of a large antarctic ice-stream controlled by tidally induced changes in the subglacial water system, *The Cryosphere*, *9*, 1649–1661, doi:10.5194/tc-9-1649-2015.

Sayag, R., and M. G. Worster (2013), Elastic dynamics and tidal migration of grounding lines modify subglacial lubrication and melting, *Geophys. Res. Lett.*, *40*, 5877–5881, doi:10.1002/2013GL057942.

Thompson, J., M. Simons, and V. C. Tsai (2014), Modeling the elastic transmission of tidal stresses to great distances inland in channelized ice streams, *The Cryosphere*, *8*,

2007–2029, doi:10.5194/tc-8-2007-2014.

Tsai, V. C. and Gudmundsson, G. H. (2015), An improved model for tidally modulated grounding-line migration, *J. Glaciol.*, *61*(226), 216–222.

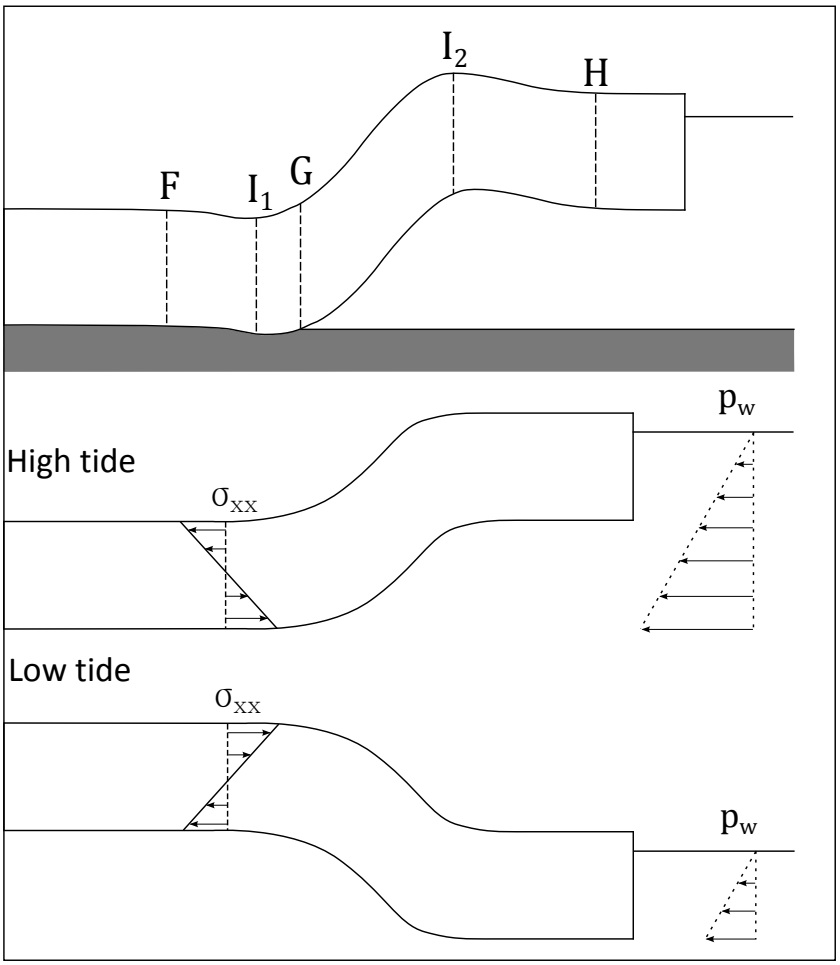

Figure 1. Schematic showing the flexural zone (top panel) defined as the region between the upstream limit of flexure (F) and the hydrostatic limit (H). The grounding line (G) lies between two inflexion points (I). In reality there are more than two inflexion points, decaying rapidly in amplitude up and downstream of the grounding line. Also shown are the flexural (σ_{xx}) and damming (p_w) stresses for high (middle panel) and low tide (bottom panel).

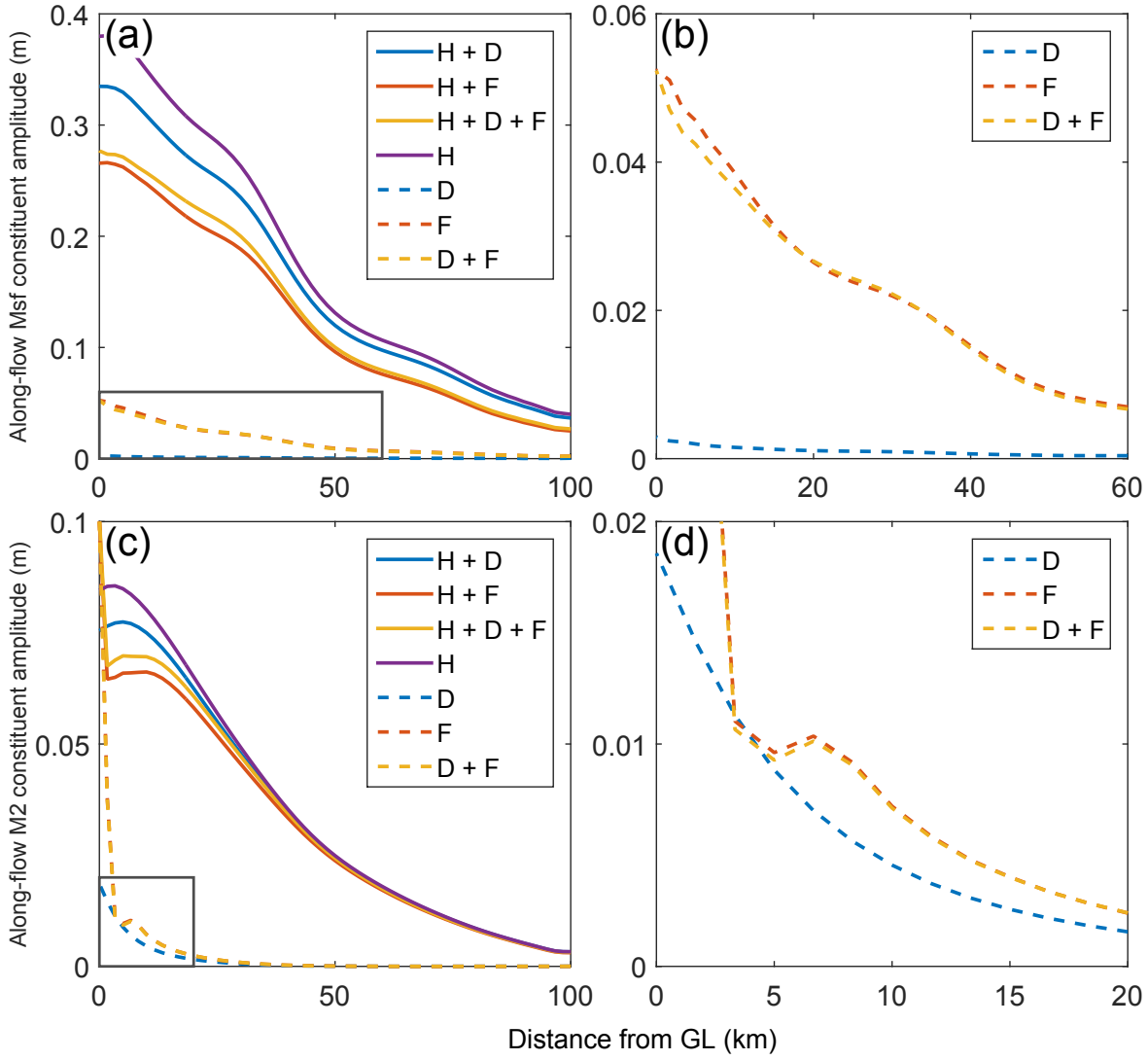

Figure 2. Amplitude of M_{sf} (top panels) and M_2 (bottom panels) frequencies plotted against distance from the grounding line, extracted from detrended horizontal surface displacements using t_tide. Different lines show the different responses when including flexural stresses (F), damming (D) or hydrology (H). The right hand panels focus in on results without hydrology (extent marked by rectangles in the left hand panels).

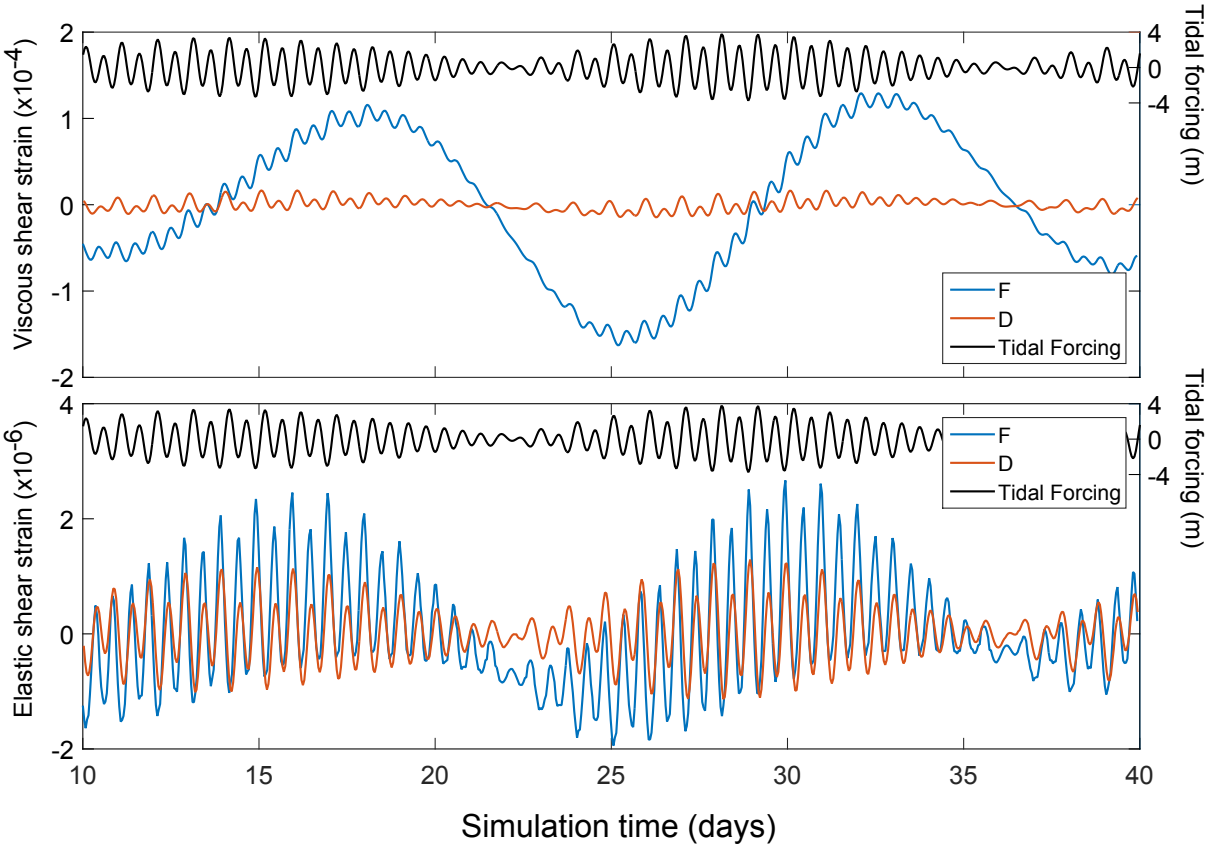

Figure 3. Viscous (top panel) and elastic (bottom panel) shear strains (ϵ_{xy}) at the ice stream bed 20km upstream from the grounding line for simulations with only flexural stresses (F) and only tidal damming (D). Tidal forcing is shown above in black.

Table 1. Parameters used in all model simulations

Parameter	**Description**	**Value**
E	Young's modulus	4.8 GPa
ν	Poisson's ratio	0.41
m	Basal stress exponent	3
q	Effective pressure exponent	10
$\bar{N}$	Mean effective pressure	110 kPa
K	Drainage system hydraulic diffusivity	$7 \times 10^9 \mathrm{m}^2\mathrm{d}^{-1}$